



8th CIRP Conference of Assembly Technology and Systems

## Towards robust human-robot mobile co-manipulation for tasks involving the handling of non-rigid materials using sensor-fused force-torque, and skeleton tracking data

David De Schepper<sup>a,1,\*</sup>, Bart Moyaers<sup>a,1</sup>, Gert Schouterden<sup>a</sup>, Karel Kellens<sup>a</sup>, Eric Demeester<sup>a</sup>

KU Leuven, Department of Mechanical Engineering, ACRO research group, Wetenschapspark 27, Diepenbeek 3590, Belgium

### ARTICLE INFO

#### Article history:

Received 30 September 2019

Revised 23 April 2020

Accepted 25 May 2020

#### Keywords:

Mobile manipulation

Force control

Human-robot collaboration

Skeleton tracking

Composites

Dry fibre sheets

Manufacturing

Sensor-based programming

### ABSTRACT

Over the past decades, robots have been extensively deployed in multiple industries. More recently, industrial robots have been taken out of their cages, being more present in dynamic, uncertain environments interacting in the vicinity of humans. Traditionally, robots have been mainly developed to perform pre-programmed tasks. However, some tasks are too complex or expensive to be performed by a robotic system alone. One of these hard tasks is the handling of large fibre sheets in composite part production. This paper presents a force-based approach towards human-robot co-manipulation of tasks involving the handling of non-rigid materials, such as composite fibres. Our approach fuses the data of a force-torque sensor and skeleton tracking data from a 2D camera to control the mobile manipulator in an intuitive manner, by using the intelligence of the operator as much as possible. By using this approach, tools such as path planning, high-level task planning, or modelling of objects to be manipulated are not essential to obtain the results. The overall approach is illustrated with a co-manipulation proof-of-concept experiment in which a mobile manipulator robot handles a flexible textile sheet together with a human operator.

© 2020 The Author(s). Published by Elsevier B.V.

This is an open access article under the CC BY-NC-ND license (<http://creativecommons.org/licenses/by-nc-nd/4.0/>)

## 1. Introduction

Robots have been extensively deployed over the last decades, as clearly indicated by statistics of the International Federation of Robotics (IFR). In 2018 for instance, investments in industrial robotics have reached a record high of USD 16.5 billion. Besides, the sale of industrial robots has augmented for the sixth consecutive year in a row. Similarly, the sales of service robots are booming and the IFR estimates that sales of all types of robots for domestic tasks could reach almost 32 million units in the period 2018–2020 (International Federation of Robotics, 2019). More recently, industrial robots have been taken out of their cages, being involved in more dynamic and uncertain environments, in the neighbourhood of and in close collaboration with humans. Traditionally, robots have been mainly deployed to perform pre-programmed tasks, e.g. painting, welding, or grasping. Many industries are making their transition towards Industry 4.0, deploying more robots in

their working areas. Certain industries however, such as the composite parts industry, still lacks flexible automation. Some branches of this industry are characterised by low-volume high-mix production scenarios. These scenarios are often found in the production processes of small medium enterprises (SMEs), where the low cost, limited complexity and high production flexibility are necessary. Robotic assistance could lead to an improvement of these characteristics, provided intuitive and fast robot reprogramming is achieved.

The process of making a composite product consists of a series of complex tasks. Some of these tasks are the transportation of fibre sheets from the cutting table or supply to the draping station, followed by selective holding during the draping process. The problem of transporting fibre sheets to a work station is twofold. Fibre sheets can be very large with surface areas exceeding one square meter, resulting in difficult handling by a single person. Moreover, non-rigid materials, e.g. carbon fibre sheets, have many degrees of freedom (DOF), which means that the sheet can wrinkle quickly resulting in a deterioration of the fibrous material.

However, in order to successfully assist the human with these complex tasks, the robot has to be equipped with additional DOF.

\* Corresponding author. Tel.: +32 11 75 17 76; fax: +32 11 27 88 21.

E-mail address: [david.deschepper@kuleuven.be](mailto:david.deschepper@kuleuven.be) (D. De Schepper).

<sup>1</sup> Authors contributed equally.

An example of these high DOF robots are mobile manipulators, which consist of a three DOF mobile platform, and a robotic arm. This paper presents a multi-modal approach towards human-robot co-manipulation of tasks involving the handling of non-rigid materials, such as composite fibres. Our approach fuses the data of a force-torque sensor and skeleton tracking data from a 2D camera to control the mobile manipulator in an intuitive manner. Our overall approach is illustrated and evaluated with a proof-of-concept experiment in which a mobile manipulator robot handles a flexible textile sheet together with a human operator.

The remainder of this paper is organised as follows. Section 2 initiates with related work concerning the human-robot collaborative manipulation of non-rigid materials. In Section 3 the problem setup is delineated. Section 4 describes the control problem. Section 5 discusses the conducted experiments and results. Finally, Section 6 concludes with a summary of this work and discusses some tracks for future work.

## 2. Related work

To be able to perform complex tasks in even more complex environments, multiple approaches are feasible. One of these complex tasks is the manipulation of non-rigid materials. These materials are used in a variety of applications and industries. Over the last couple of years, the manipulation of (non-)rigid materials has gained increased interest for use in various industrial applications, e.g. laundry and clothing folding, automotive, and manufacturing industry (Rizzi et al., 2000). In order to perform this complex task, a robot has to plan a trajectory in advance. However, performing such computations can quickly become very time consuming, thus hard to execute in real time (Miller et al., 2012). These computations can, however, be mitigated by having a *human-in-the-loop* system. This way the computational load is reduced since the high-level trajectory planning is performed by the operator, while the robotic system reacts –in an intuitive manner– to the state of the human, the co-manipulated object, or the environment.

Human-robot object (co-)manipulation has gained enormous interest. Vanthienen et al. demonstrated robot wrench control, i.e. force and torque control, on a PR2 robot for force-sensor-less robot tasks (Vanthienen et al., 2012). The authors extended the iTaSC framework and applied their approach to the human-robot co-manipulation task of a robot carrying a plate in a restaurant while avoiding obstacles and maintaining visual contact with a human. Although this approach scaled well with rigid materials, the control loop might not be efficient for deformable objects, because non-rigid materials, such as fabrics, cannot transfer compressive forces. Research towards automated manipulation of flexible materials has gained interest as well. Miller et al. demonstrated robotic laundry folding based on a quasi-static cloth model (Miller et al., 2012). The authors used the PR2 robot for folding a long-sleeved shirt. The state of the shirt was monitored using a depth camera. Lee et al. used a machine learning algorithm to learn the optimal trajectory for manipulating non-rigid materials (Lee et al., 2015). The authors demonstrated their trajectory-aware non-rigid approach on several challenging tasks, including the folding of towels and grasping objects in a bin. Bodenhausen et al. used an adaptable vision system towards the manipulation of flexible objects in an industrial environment, including peg-in-hole tasks and laying-down actions (Bodenhausen et al., 2014). Human-robot manipulation of highly deformable materials in a collaborative manner has been examined by Kruse et al. (2015). The authors showed that a hybrid control loop combining force and vision data outperformed a force controller. As input for the vision-based controller, a RGB-d camera was applied to capture the state of the cloth. Intentions of the human manipulating the cloth was estimated based on an approximate, discrete cloth model. Simulations

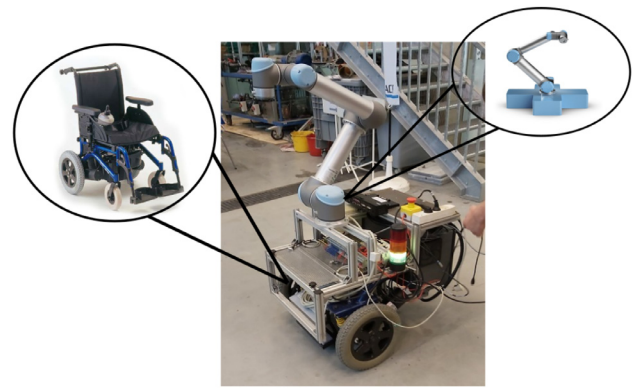


**Fig. 1.** The AMBER mobile manipulator. AMBER is an abbreviation for **ACRO MoBile platform Extended with Robotic arm**, a multi-purpose mobile manipulator robot for research and education. AMBER consists of a non-holonomic three degrees of freedom mobile wheelchair platform from Invacare, and a six degrees of freedom Universal Robots UR5 collaborative robotic arm.

in a physics engine environment showed satisfactory results. Redundancy in the kinematic chain of the mobile manipulator was resolved by solving an optimisation problem based on equality constraints (Kruse et al., 2017). As a mobile manipulator, the authors used the Baxter-on-Wheels platform, a mobile manipulator consisting of two 7-DOF compliant robotic arms, and a 3-DOF non-holonomic wheelchair base. Although the approach showed good results in a simulation environment, it is not clear whether the approach also performs well in a real-life environment with unintended disturbances, e.g. uncertainties regarding sensors, actuators, and the environment itself.

Our approach to co-manipulating non-rigid materials is related to the work of Kruse et al. (2015, 2017). Monitoring the cloth could cause the algorithm to erroneously estimate the state of the material due to environmental uncertainties, e.g. light conditions, or reflections from a composite fibre sheet. However, instead of estimating the state of the non-rigid material, we estimate the intentions of the human by monitoring the pose relative to the centre of the manipulated cloth. 2D images from a camera are input for a hybrid force vision controller. We evaluate our approach with a real-life proof-of-concept test case.

## 3. Robot platform

The robot platform used in this work is the **ACRO mobile platform extended with robotic arm** abbreviated to AMBER, depicted in Fig. 1. AMBER is a modular, and multi-purpose mobile manipulator designed and built for research and education purposes. As can be seen, AMBER consists of two main components; a modified, non-holonomic, three DOF Invacare wheelchair base from Dynamic Controls, and a six DOF industrial collaborative robotic arm from Universal Robots (UR5). To control the mobile platform, the original joystick of the electric Invacare wheelchair was modified to accept analog computer signals allowing to control the speed and rotation of the platform. For safety reasons, AMBER can be remotely stopped by pressing an emergency button. The differentially driven wheelchair base fits to the kinematic unicycle robot model:

$$\begin{pmatrix} \dot{x} \\ \dot{y} \\ \dot{\theta} \end{pmatrix} = \begin{pmatrix} \cos(\theta) & 0 \\ \sin(\theta) & 0 \\ 0 & 1 \end{pmatrix} \cdot \begin{pmatrix} v \\ \omega \end{pmatrix} \quad (1)$$

where  $\dot{x}$ ,  $\dot{y}$ , and  $\dot{\theta}$  represent the 3-DOF velocities in the world frame, and  $v$ ,  $\omega$  the linear and rotational velocity of the robot frame.

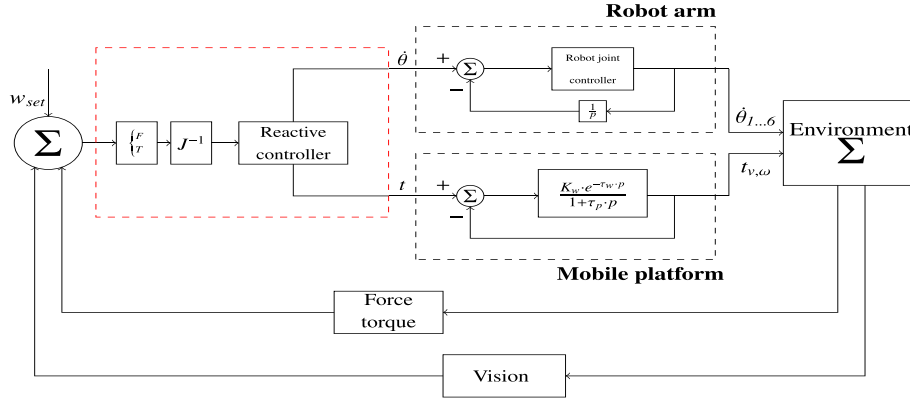


Fig. 2. Diagram of the hybrid force-vision control loop. All computations are run on-line. The red dashed rectangle points out the force-vision controller. Redundancy in the kinematic chain of the mobile manipulator is solved using two parallel controllers (dashed rectangles in black), one for the robotic arm and another one for the mobile platform.

#### 4. Robot control

Instead of monitoring the state of the non-rigid material, carried by the robot and the human operator, our approach aims to measure a wrench, i.e. a force and a torque, at the end effector frame of the mobile manipulator (Baeten et al., 2003). Our approach uses a hybrid force-vision feedback control loop to minimise the error wrench induced by the human operator while transporting the non-rigid material. Since the object to be manipulated is deformable, a stand-alone force control loop will not work sufficiently enough due to the characteristics of the non-rigid material, as explained by Kruse et al. (2015). The entire hybrid force-vision control loop is depicted in Fig. 2.

##### 4.1. Impedance controller

At each time step  $t$ , a six-axis force-torque Robotiq<sup>®</sup> sensor extracts wrench signals induced by the human operator on the deformable material. This wrench signal  $\mathbf{w}$  is expressed by a six-dimensional vector containing the forces and torques in 3D Cartesian space:

$$\mathbf{w} = [F_x \ F_y \ F_z \ M_x \ M_y \ M_z]^T \quad (2)$$

At time step  $t_0$ , the human operator can set the desired (linear) stretching task frame force  $\mathbf{F}_{set}$  by holding the deformable object with a desired stiffness. The six-axis force-torque sensor is calibrated at the set stretching force. Wrench signals  $\mathbf{w}$  are then captured at a fixed frequency  $f$  of approximately 100Hz. Inverse dynamics of the kinematic chain of the robotic manipulator is used to calculate the angular velocity of each joint of the robot:

$$\mathbf{F}_{EE} = \mathbf{J}(\theta) \cdot \mathbf{F}_q \quad (3)$$

$$\dot{\theta} = \mathbf{J}(\theta)^{-1} \cdot \dot{\mathbf{x}} \quad (4)$$

$$\dot{\mathbf{x}}_{EE} = \mathbf{C} \cdot \mathbf{F}_{EE} \quad (5)$$

where  $\mathbf{F}_{EE}$  represents the forces at the end effector,  $\mathbf{F}_q$  torques of each joint of the kinematic chain,  $\mathbf{J}$  the Jacobian Matrix, which gives the relation between end-effector (EE) forces and joint torques,  $\dot{\theta}$  a vector of robot joint velocities, and  $\dot{\mathbf{x}}$  a vector of 3D Cartesian velocities in the robot base frame. First the EE frame's desired velocities are calculated from the measured forces and torques in the EE according to Eq. (5) where  $\mathbf{C}$  is a constant. We then calculate the desired robot joint velocities for a given EE frame velocity using the inverse of the Jacobian matrix (Eq. (4)). Fast calculation of the Jacobian is performed using the Kinematics and Dynamics Library

from the OROCOS project (Bruyninckx, 2001; Smits, 0000). This results in a controller which reacts in a reactive manner to forces and torques induced at the task frame by sending joint velocities to the robot controller.

$$\mathbf{p} = [x \ y \ z]^T \quad (6)$$

$$\mathbf{p}_{diff}(t) = \mathbf{p}_t - \mathbf{p}_0 \quad (7)$$

$$F_{virt} = K \cdot \|\mathbf{p}_{diff}\| \quad (8)$$

$$q_{diff}(t) = \frac{q_t}{q_{t-1}} \quad (9)$$

$$T_{virt} = k \cdot \text{angle}\left(\frac{q_{diff}}{\|q_{diff}\|}\right) \quad (10)$$

At time step 0, the EE frame is located at a fixed position with Cartesian coordinates  $\mathbf{p}_0$  consisting of 3 Cartesian coordinates and a quaternion for rotation as shown in Eq. (6). When the operator induces a force and torque on the end effector at time step  $t$ , the EE frame will move to a new position  $\mathbf{p}_{t+1}$ . The vector difference  $\mathbf{p}_{diff}$  (see Eq. (7)) is used to calculate an artificial *extra* force  $F_{virt}$  pushing the EE back to its equilibrium position  $\mathbf{p}_0$ . A similar approach has been used to calculate the necessary reactive torques pushing the arm's EE back to the start pose. Using the angle-axis representation of the quaternion difference  $q_{diff}$  shown in Eq. (9) a virtual torque vector  $\mathbf{T}_{diff}$  can be calculated using Eq. (10). The parameters of the impedance controller can be set, i.e. the linear ( $\frac{N}{m}$ ) and rotational ( $\frac{N \cdot m}{rad}$ ) stiffness of the compliant impedance controller.

##### 4.2. Skeleton tracking

In parallel to the wrench control loop, an Intel RealSense 3D stereo vision camera (of which currently only the 2D RGB image data are used) captures images at a fixed frame rate. The camera is used to estimate the intentions of the operator carrying the non-rigid material by tracking the skeleton of the human operator. For key point tracking in 2D images, we use the skeleton tracking package OpenPose (Cao et al., 2018; Simon et al., 2017). In the vision control loop, poses of the operator's key points relative to the center of the manipulated cloth are extracted. Several key points are captured, such as the operator's wrists, shoulders, ears, eyes and nose. These key points are also the ones used to estimate the intentions of the operator. Fig. 3 shows the output of the skeleton tracking algorithm used to estimate the intentions of the operator. Our approach gives the first priority to the wrist key points of the

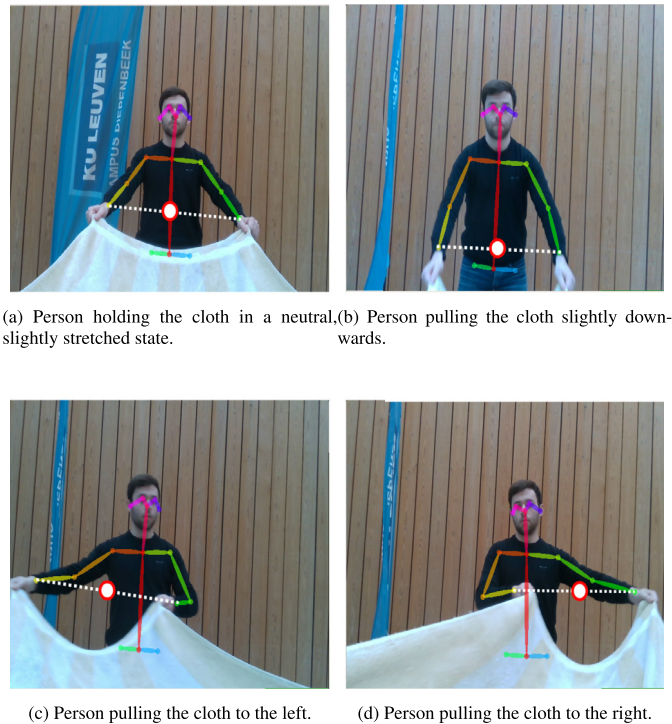


**Fig. 3.** Illustrations of the OpenPose skeleton tracking algorithm by Cao et al. (2018); Simon et al. (2017). Wrists, shoulders, ears, eyes, and nose are the key points used to estimate the intentions of the human operator. The midpoint between the wrist key points is represented in the red-white dot.

operator, since he has to hold the deformable object and has to manipulate it. The midpoint between the left and right wrist key-points is calculated. The distance  $d$  between this midpoint and the exact center of the camera frame is used to calculate a virtual force  $F_v$  according to the following equation:  $F_v = K \cdot d$ . This virtual force in turn moves the robot. Fig. 3a depicts the equilibrium pose of the human operator, captured by the camera. Figs. 3b, 3c, and 3d show the human pulling the cloth slightly downwards, to the left, and to the right respectively. When the wrist key points cannot be tracked, the approach is applied on the shoulders, eyes, or ears.

### 4.3. Potential field control

We now have a hybrid, reactive control loop performing compliant impedance control based on force and torque measurements, and executes visual servoing based on skeleton tracking data. This hybrid force-vision control loop performs robustly in co-manipulating a deformable object. However, to ensure that the mobile manipulator uses its manoeuvrability, i.e. all its DOF, we introduce the potential field reactive control principle, an intuitive reactive controller which can handle redundancy in the kinematic chain. The principle of this intuitive, reactive controller is as follows. At time stamp  $t_0$ , the mobile manipulator is in its equilibrium state, facing the human operator. When the operator wants to co-manipulate the cloth by pulling it to the desired direction, the hybrid force-vision controller reacts robustly to this change and wants to minimise this error by reacting compliantly to ensure that the EE frame of the robot is in the centre of the 2D image. Due to the deviation of the human operator, an artificial, repellent force,  $F_{virt}$  is induced. This virtual force is felt by the mobile platform of the robot. This force is the trigger to command the mobile platform to move. The controller reacts to this force by sending a velocity to the mobile platform proportional to the repellent force. While the platform is moving, the repellent force at the EE frame, induced by

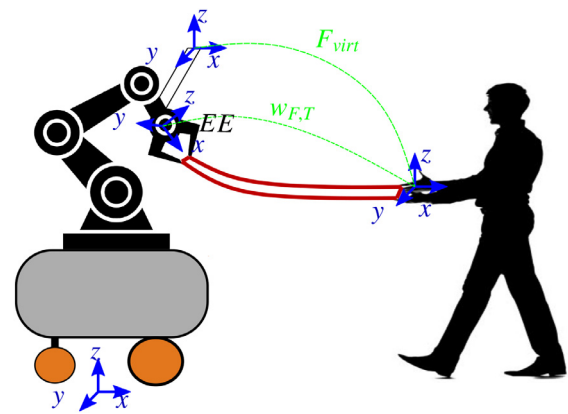


**Fig. 4.** Experimental setup of the co-manipulation task of transporting a flexible, non-rigid composite fibre sheet to a workplace.  $W_{F,T}$  represents the induced wrench (force and torque) by the human, captured by the six-axis force torque sensor at the end effector frame,  $EE$ , of the robot arm.  $F_{virt}$  represents the artificial force induced by the human, captured by the 2D camera mounted on the end-effector of the robot.

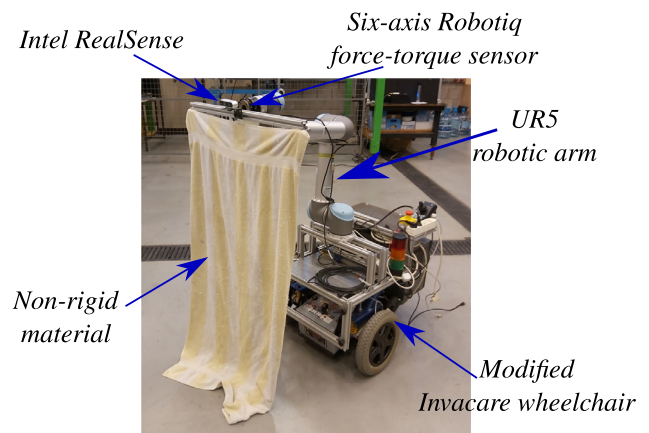


**Fig. 5.** Setup showing an adapted AMBER equipped with a six-axis force-torque sensor from Robotiq<sup>®</sup> placed in the end-effector of the Universal Robots UR5 robotic arm, a self-designed end-effector tool for holding the non-rigid material during task execution, and a RealSense<sup>®</sup> 3D camera from Intel mounted on top of the end-effector tool.

the human operator, will decrease, and the whole system stabilises around the equilibrium state. Through this intuitive manner of controlling a mobile manipulator, redundancy in the kinematic chain is solved. In this approach, the robot arm gives first response, while the mobile platform follows secondly when a repellent force at the EE frame is induced. This approach is illustrated in Fig. 4. The force-torque sensor, mounted on the end effector of the industrial, collaborative robot, measures the induced wrench of the human operator on the cloth. The camera monitors the key points of the operator, and performs the feedback for the visual servoing, and captures the artificial, repellent force induced on the mobile manipulator by deviating from the equilibrium state. Fig. 2 depicts the entire hybrid force-vision control loop with intuitive reactive velocity controller. The environment produces forces, torques, and deviations. The overall control loop tries to minimise these by using a proportional, reactive velocity controller (depicted in the red, dashed rectangle). This controller maps forces and torques to joint velocities  $\dot{\theta}$  for the robotic arm, and a twist  $\mathbf{t}_{v,\omega}$ , which comprises the linear and rotational velocity for the mobile platform. These commands are sent to the UR5 robot joint controller, and the wheelchair's base controller. The output of the wheelchair's controller is a filtered, delayed linear and rotational velocity.

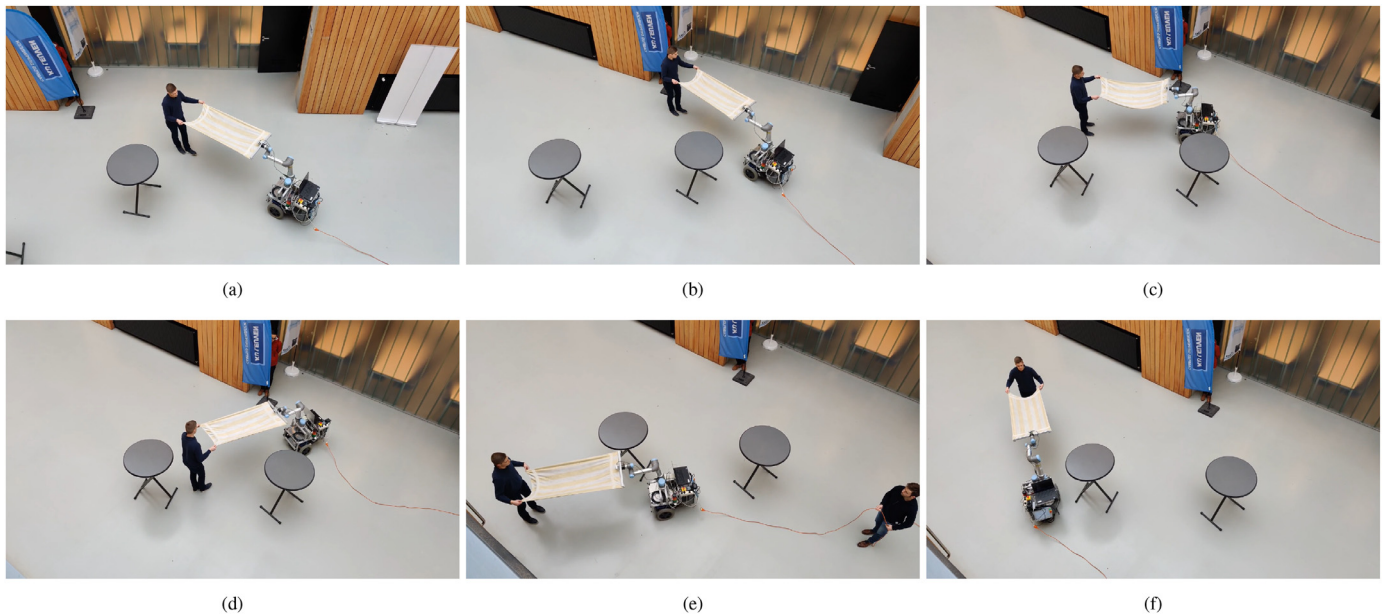


**Fig. 6.** Selected frames from running the reactive, hybrid force-vision controller in a key task involving the collaborative human-robot transportation of a deformable object. The objective of the mobile manipulator is to follow the intentions ordained by the human operator. To test the robustness of the controller, the human operator has to guide the mobile manipulator in between two obstacle. *w*Fig. 6a shows the starting point. Fig. 6b depicts the first turning point. Fig. 6c shows the tipping point where the robot has to move backwards to hold the non-rigid object at desired stiffness. Fig. 6d depicts the moment where the robot reacts on the operator's intention, and moves forwards. Fig. 6e shows the second turning point where the trajectory is changed. Finally, figure 6f depicts the end point of the task.

## 5. Experimental results

To evaluate our hybrid reactive controller, five main experiments<sup>2</sup> were conducted. These experiments include the evaluation of a pure force-torque reactive control, a pure vision control using skeleton tracking, backwards parking, manoeuvring around a corner, and a task in which a mobile manipulator robot handles a non-rigid textile sheet together with an operator, transporting the sheet from one work station to another. The latter experiment is discussed in this section. For testing purposes, some adjustments have been made to our mobile manipulator robot AMBER, as can be seen in Fig. 5. All simulations were run in a Linux environment (Ubuntu 18.04 LTS) on a laptop with Intel® Core™ i7-8750H CPU @ 2.20GHz and 16 GB RAM. The reactive controller is implemented in the Robot Operating System (ROS), using the Universal Robots UR5 and Robotiq® Force/Torque sensor drivers (Quigley et al., 2009).

Fig. 6 depicts several time frames captured during execution of the collaborative mobile transportation task of a composite fibre sheet. At time step  $t = 0$ , the human operator will set the desired fibre tension by applying the correct force at the EE frame, as can be seen in figure 6a. Next, the human operator will start guiding the mobile manipulator from one work station towards the next work station. During this event, the human operator will perform a slalom between two obstacles (physically represented by two folding tables). Fig. 6b depicts the moment where the operator will start to manoeuvre through the two obstacles. At first glance, the operator takes his corner widely (Fig. 6c), he therefore has to guide the robot backwards to make the corner (Fig. 6d). Fig. 6e shows the operator forcing the robot to make the corner towards the end point, depicted in Fig. 6f.

<sup>2</sup> Footage of these experiments can be retrieved on our YouTube channel through following link: <https://youtu.be/tOXUz4Fo-qM>.

## 6. Conclusion and future work

This paper presents an overall approach towards human-robot mobile co-manipulation for tasks involving the handling of non-rigid materials. In addition, our approach could potentially be applied to rigid materials as well. In the proof-of-concept experiments, the hybrid force-vision reactive controller using skeleton tracking feedback, demonstrated satisfactory results concerning the transportation of a deformable composite fibre sheet from one work space to another, in the absence of modelling the state of the object. However, during the proof-of-concept experiments we have noticed that the controller can become unstable when the operator performs a sinusoidal movement. The reactive controller, with good tracking behaviour, follows well, but will generate an unstable oscillation in joint, linear, and rotational velocity. Above that, something that misses in the current implementation is an intuitive way to translate the mobile platform sideways, around the operator. Future work concerns the further tuning and testing of the reactive controller for better, intuitive performance. The potential of using 3D vision data will be explored. Additionally, an online obstacle avoidance inference scheme will be added to avoid collisions with obstacles while executing an obtained task. In future work we additionally aim to integrate this work into the eTaSL (Expression-graph Task Specification Language) framework of our department for instantaneous robot task specification and control (Aertbeliën and De Schutter, 2014).

## Acknowledgments

The authors gratefully thank KU Leuven, Diepenbeek Campus, for granting a FLOF mandate, facilitating this research. Bart Moyaers is a Baekeland (Flanders Innovation & Entrepreneurship) PhD fellow under grant agreement HBC.2019.2222. The authors would also like to thank the researchers of KU Leuven research groups ACRO for their contributions to the construction of the mobile platform.

## References

- Aertbeliën, E., De Schutter, J., 2014. eTaSL/eTC: A constraint-based task specification language and robot controller using expression graphs. In: 2014 IEEE/RSJ International Conference on Intelligent Robots and Systems, pp. 1540–1546.
- Baeten, J., Bruyninckx, H., Schutter, J.D., 2003. Integrated Vision/Force Robotic Servicing in the Task Frame Formalism. *The International Journal of Robotics Research* 22 (10-11), 941–954.
- Bodenhagen, L., Fugl, A.R., Jordt, A., Willatzen, M., Andersen, K.A., Olsen, M.M., Koch, R., Petersen, H.G., Kruger, N., 2014. An Adaptable Robot Vision System Performing Manipulation Actions With Flexible Objects. *IEEE Transactions on Automation Science and Engineering* 11 (3), 749–765.
- Bruyninckx, H., 2001. Open robot control software: the OROCOS project. Institute of Electrical and Electronics Engineers, pp. 2523–2528.
- Cao, Z., Hidalgo, G., Simon, T., Wei, S.-E., Sheikh, Y., 2018. OpenPose: realtime multi-person 2D pose estimation using Part Affinity Fields. arXiv preprint arXiv:1812.08008.
- International Federation of Robotics, 2019. Industrial Robots: Robot Investment Reaches Record 16.5 billion USD.
- Kruse, D., Radke, R.J., Wen, J.T., 2015. Collaborative human-robot manipulation of highly deformable materials. In: 2015 IEEE International Conference on Robotics and Automation (ICRA), pp. 3782–3787.
- Kruse, D., Radke, R.J., Wen, J.T., 2017. Human-robot collaborative handling of highly deformable materials. In: 2017 American Control Conference (ACC), pp. 1511–1516.
- Lee, A., Gupta, A., Lu, H., Levine, S., Abbeel, P., 2015. Learning from Multiple Demonstrations using Trajectory-Aware Non-Rigid Registration with Applications to Deformable Object Manipulation. In: Proceedings of the 28th IEEE/RSJ International Conference on Intelligent Robots and Systems (IROS).
- Miller, S., van den Berg, J., Fritz, M., Darrell, T., Goldberg, K., Abbeel, P., 2012. A geometric approach to robotic laundry folding. *The International Journal of Robotics Research* 31 (2), 249–267.
- Quigley, M., Conley, K., Gerkey, B.P., Faust, J., Foote, T., Leibs, J., Wheeler, R., Ng, A.Y., 2009. ROS: an open-source Robot Operating System. ICRA Workshop on Open Source Software.
- Rizzi, C., Bordegoni, M., Frugoli, G., 2000. Simulation of Non-Rigid Materials Handling, pp. 199–210.
- Simon, T., Joo, H., Matthews, I., Sheikh, Y., 2017. Hand Keypoint Detection in Single Images using Multiview Bootstrapping. CVPR.
- Smits, R., KDL: Kinematics and Dynamics Library. <http://www.orocos.org/kdl>.
- Vanhienen, D., De Laet, T., Bruyninckx, H., Decré, W., De Schutter, J., 2012. Force-Sensorless and Bimanual Human-Robot Comanipulation Implementation using iTaSC. *IFAC Proceedings Volumes* 45 (22), 759–766. 10th IFAC Symposium on Robot Control